MEASUREMENTS OF MOMENTUM HALO DUE TO THE REDUCED RFQ VOLTAGE DURING THE LIPAc BEAM COMMISSIONING

K. Hirosawa*, A. De Franco, K. Masuda, A. Mizuno, S. Kwon,
K. Kondo, M. Sugimoto, K. Hasegawa, QST, Rokkasho, Japan
I. Moya, F. Scantamburlo, F. Benedetti[1], D. Gex, H. Dzitko, Y. Carin, F4E, Garching, Germany
I. Podadera[2], J. C. Morales Vega, IFMIF-DONES España, Granada, Spain
[1]also at CEA, France
[2]also at CIEMAT, Madrid, Spain

Abstract

The Linear IFMIF Prototype Accelerator, LIPAc, is being commissioned aiming at validating the RFQ up to 5 MeV beam acceleration. Eventually, the nominal beam of 5 MeV-125 mA in 1 ms length and 1 Hz rate pulsed mode was achieved in 2019. The beam operation has been resumed since July 2023 after long maintenance including recovery from unexpected problems in the RFQ RF system. This new phase aims at the commissioning of the full configuration except SRF linac, which is replaced by a temporary beam transport line. Focusing on the RFQ behaviour, it will be interesting to operate it at higher duty especially for longer pulses. Indeed, a beam simulation study suggested that the beam extracted from the RFQ includes considerable momentum halo when the vane voltage reduces by more than 5 percent, with a slight decrease of mean energy. It can be a potential source of quench like the mismatched beam in the cryomodule. This could be studied measuring the energy from the Time-of-Flight among multiple BPMs while monitoring beam loss around the dipole, where momentum halo should be lost. During the upcoming commissioning in the present Phase, we propose to study them by scanning the RFQ voltage.

INTRODUCTION

LIPAc The Linear IFMIF Prototype Accelerator) is the accelerator to validate low energy part up to 9 MeV where the space charge dominant region of the design of the International Fusion Material Irradiation Facility (IFMIF), which is the accelerator-based neutron source for the test facility of the materials for the fusion reactor. carried out in Rokkasho, Aomori, Japan, under the collaboration framework between EU and Japan [1]. The system, in the design, is aiming to accelerate the 125 mA deuteron beam with continuous wave (CW) [2]. We are now in the stage of intermediate of the full commissioning, called as Phase-B+ [3], which is positioned between the Phase-B, RFQ acceleration, and the Phase-C, superconducting RF linac [4] and the high-power beam dump [5].

We had a beam commissioning to validate the system RFQ acceleration with the low energy beam dump, 125 mA, 1 ms pulse is successfully accelerated in 2019 [6]. Most of the accelerator construction has been done by in kind contri-

bution of EU facilities until 2021. Remaining component toward to full specification is the cryomodule linac, which can accelerate the beam from 5 MeV to 9 MeV. While preparation of superconducting linac to fix some issues found during construction, the beam operation was started in June of 2021 [7]. RFQ commissioning to be reached to CW had been also performed, but then the destructive sparks are happened in the transition part of a circulator, used to protect the tetrode system from the reflection power. During the following optional challenge to drive RFQ with 7 of 8 RF stations, vacuum leak from RF input couplers had been observed. As above two events became the decisive damage of our RFQ-RF system, we moved to a long maintenance term to recover the system over one year. The beam commissioning has been resumed from July of 2023 [8-10].

In this report, we share our progress of the beam commissioning, concentrating on the proceeding of the RFQ beam commissioning diagnosed by using beam position and phase monitors (BPMs) [11, 12] with the improved digitizer unit and beam loss monitors (BLoMs) [13, 14], which are ionization chambers and 3He detectors, positioned along newly constructed downstream transport up to the large beam dump.

LIPAc STATUS

Overview of the LIPAc Phase-B+

The Phase-B+ stage of our LIPAc has only RFQ cavity as the accelerating component. Downstream part consists of beam transport section with several beam diagnostics and the large beam dump as the new feature from this commissioning phase. Bridge section called MEBT Extension Line (MEL) between MEBT and HEBT instead of the cryomodule linac, is temporary inserted specifically in this commissioning phase.

The Stage-1 beam commissioning was performed with much low current beams of 10 mA H+, as the test, and 20 mA D+. For the ion source part, a 6 mm φ small extraction aperture was adopted. We could observe the 20 mA transmission up to the beam dump with chopped 100 μs beam in 1 Hz repetition rate. The purpose of this stage is checking the alignment of newly installed components and functionality of each diagnostic, to prepare coming high current and high duty beam operation and the beginning stage of Phase-C commissioning. We found some issues for diagnostics, espe-

---

* hirosawa.koki@qst.go.jp

cially in BPM and interceptive devices including multi-wires beam profile monitor. Beam time was limited, but we confirmed the alignment errors and quasi lossless transmission to the beam dump. While RFRFQ part maintenance, injector conducted the CW commissioning with 165 mA total extract current [15]. Developed reliability of the injector condition is also one of new feature of present commissioning phase.

The Stage-2 beam commissioning aims to transport the nominal 125 mA D+ beam by using a 11.5 mm φ plasma electrode, with low duty cycle managed by chopper system. The advantage of this stage is applicability of the interceptive devices consisting of horizontal and vertical slit scanners, multi-wires beam profile monitors, and a faraday cup. Regarding the preparation of non-interceptive devices consisting of BPMs, several residual gas monitors, and BloMs for the higher duty operation, crosscheck is being conducted. In the Stage-3, all interceptive devices will be extracted in normal, and duty cycle will be increased toward CW [13]. Because our chopper system is limited to use 3 ms pulse with 10 Hz repetition rate in maximum from injector RF source point of view, so this stage includes to switch beam handling from chopped beam to raw extracted beam.

As the general result of the operation, we have achieved 90 percent beam transmission down to the BD in ACCTs, shown in Fig. 1. From the intensity point of view, from 30 µs part looks plateau. Even in that plateau, we observed that the centroid position, shown in Fig. 2, was modulated by changing space charge neutralization in several Kr gas flow rates to the injector. It is also interesting topic under studying in this commissioning phase.
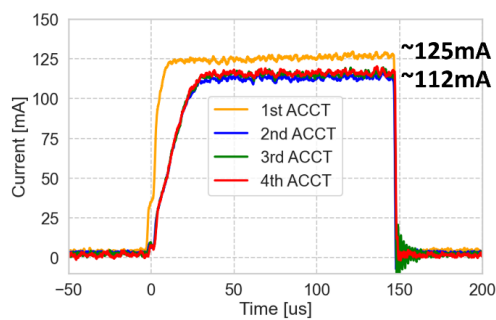
Figure 1: Waveform of the ACCTs with 60 µs chopper gate ≈125 mA in LEBT and ≈112 mA in RFQ exit and downstream CTs.
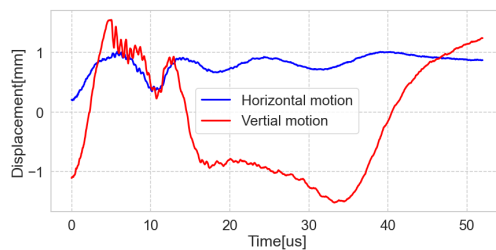
Figure 2: Intra-pulse centroid motion for the 60 µs pulse averaged over 30 shots measured by BPM installed in the medium point of the MEL.

Importance to Evaluate Momentum Halo

For the superconducting cryomodule, frequent quench caused by particle losses is one of typical failure modes of beam transmission. According to the design report of LIPAc superconducting linac, particle loss along one cryomodule should be limited to 10 W from cooling capacity point of view of the 4 K helium tank [16]. Because behaviour of the local hot spot is unclear, so discussion of losses in this report is conducted in the total heat.

Present LIPAc and original IFMIF accelerator designs, energy filter is not implemented. Momentum halo, which is distributed out of acceptable region, can be directly coming to the cryomodule. We are discussing to insert the energy filter like chicane or dog leg type transport, for the future accelerator. Here, from LIPAc operational point of view, the way to measure and watch existence of momentum halo due to the reduced RFQ vane voltage is considered. The reduced voltage can be appeared in the beam operation because of imperfect cavity pickup transmission. Dynamic effect, like thermal, in the pickup and transmission line or noise environment surround diagnostic and control modules can disturb accuracy of the read voltage of the RFQ cavity field. This uncertainty is also included in the calibration value.

BEAM SIMULATION STUDY

RFQ Simulation by Toutatis in TraceWin

The low energy beam transport after acceleration column consists of two steering and solenoid magnets, the emittance meter unit, and the repeller cone electrode. The chopper unit is also implemented between two solenoids, and it can be switched with the emittance meter unit depending on the injector operation mode. One of features of this beam commissioning phase is to test the functionality of the chopper system. Schematic layout of the LEBT and RFQ section is illustrated in Fig. 3.
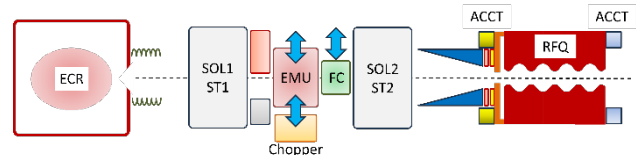
Figure 3: Layout of LEBT and RFQ section of LIPAc.

The simulation and experimental report of LEBT transmission is published by L. Bellan with the result of injector commissioning [17]. According to the report, space charge compensation in the LEBT part is very strong without chopper. The simulated and measured result described in the paper for the transverse particle distribution at the emittance meter unit is near parabolic. Thus, following values listed in Table 1 are used in simulations.

In the calculation, to avoid unexpected non-uniform distribution on the longitudinal plane, RFQ input beam is once reproduced by using calculated transverse Twiss parameters and emittances at the entrance of the cavity, shown in Fig. 4.

Table 1: Simulations Input Parameters

Parameter	Value
Beam Parameters	
Beam energy	100 keV
Extract beam current	140 mA as D+ beam
Transverse distribution	Parabola with 2.8 sigma
Twiss Parameters	
Beta at EMU	15 mm / (π·mrad)
Alpha at EMU	0.55
RMS emittance	0.25 π·mm·mrad
RMS energy spread	5×10^{-5} MeV
Other Conditions for Calculation	
Frequency of RFQ-RF	175 MHz
Space charge comp. factor	0.98
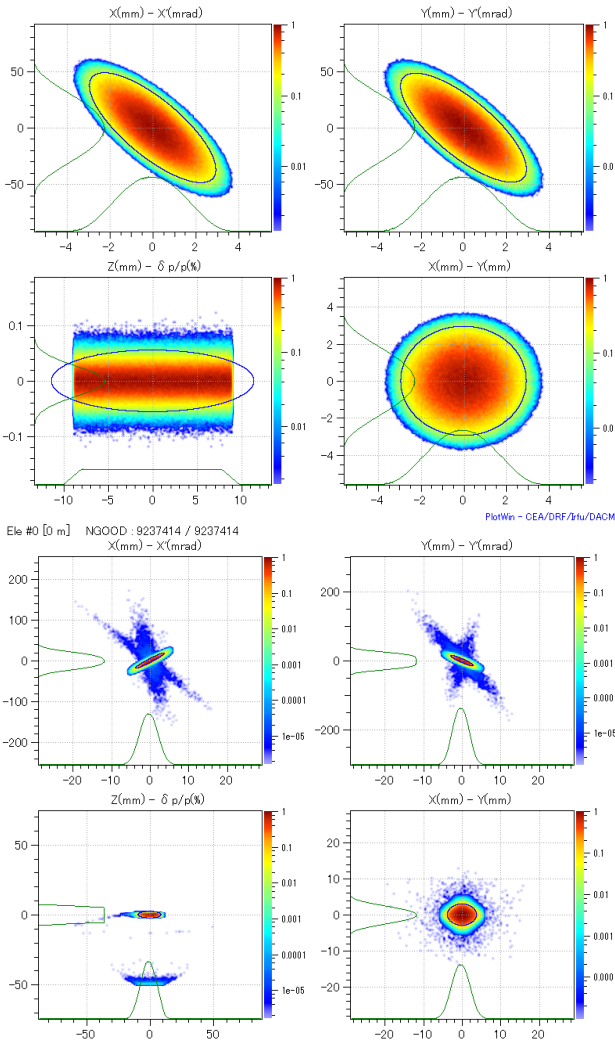
Figure 4: Initial (upper) and typical RFQ exit (lower) distributions of the RFQ simulation with nominal vane voltage: 132 kV.

With keeping the initial condition, transported distributions for several vane voltages of the RFQ were calculated by using the TraceWin and Toutatis particle tracking simulations. The results for longitudinal varieties are listed

in Fig. 5. Voltages were changed from 90 percent to 105 percent of the nominal voltage of the design: 132 kV. We are now using 13 kV for the beam operation as the new operation setting from transmission point of view shown in Fig. 6, and our interesting is potentially beam loss during the beam operation because of the reduced voltage from 138 kV, which is a bit larger voltage of setting, to 119 kV, to study bunch distribution on the energy direction. Especially from the 98 percent voltage, a tail of momentum halo is started to be increased, and second energy level is appeared from 95 percent. Depending on the RFQ geometric pattern, output beam is modified in discrete on the ordinate (Energy). Figure 7 shows density distributions of energy in the logarithmic scale. Several lower energy level particles are distributed widely in the bunch. and 5 MeV and 100 keV, which is not accelerated particles, are gathered near centre of the bunch.
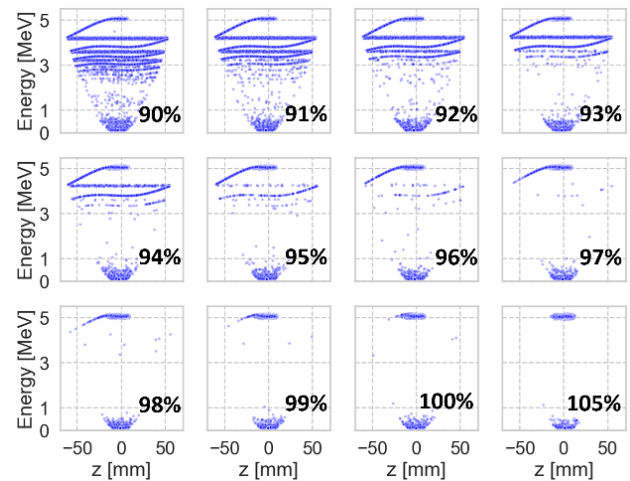
Figure 5: Longitudinal distributions for several RFQ vane voltages from 90 percent (=119 kV) to 105 percent (=138 kV), started from the same initial distribution.
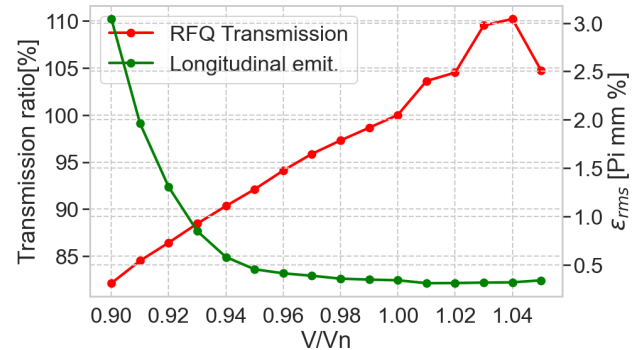
Figure 6: RFQ vane voltage vs normalized transmission of RFQ (red, ordinate of the left side), and normalized longitudinal RMS emittance (green, ordinate of the right side).

If we assume that non-accelerated and different energy level particles are not detected by our BPMs system, we must evaluate the mean energy in 1 keV resolution to discern each RFQ voltage. Figure 8 is the plot for the mean energy of all particles in one bunch bucket (blue) and only 5 MeV
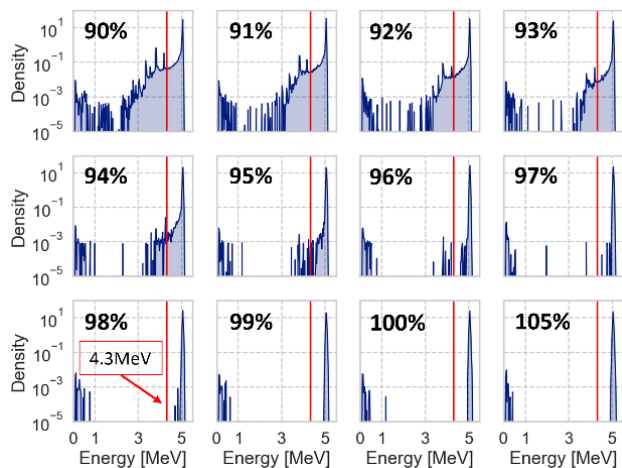
Figure 7: Distribution of the density plot for several RFQ vane voltages from 90 percent (=119 kV) to 105 percent (=138 kV), started from the same initial distribution.

energy level particle, which looks detectable as the same batch even in downstream part.
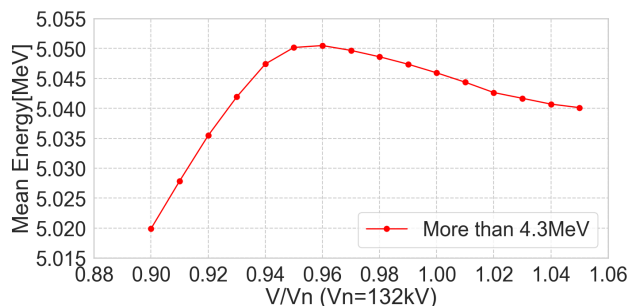
Figure 8: RFQ voltage vs mean energy, more than 4.3 MeV.

Transport Simulation by TraceWin

Concern of the existence of numerous momentum halo is mainly hot spot in the superconducting surface. Lattice design and the transmission of the envelop for Phase-C and Phase-B+ are illustrated in Figs. 9 and 10, respectively. The section of 2.3—7.8 m from entrance of the MEBT is the part of the cryomodule, and we require to make particle loss integrated along the section less than 10 W. To avoid unexpected thermal quench because of momentum halo, it is important to get a way to watch the RFQ voltage reduction. We consider having crosscheck between BPMs and BLoMs measurement if monitoring can be realized.

Loss part in the cryomodule for several RFQ voltages is drawn in Fig. 11. Upper figure denotes the variation from 90 percent to 105 percent of RFQ voltage, and lower denotes more focusing plots from 95–105 percent. From this result, less than 94 percent of nominal RFQ voltage has some quench risk.

For the measurement in this commissioning phase, detectable losses along the beam line including the downstream component are considered, because it is good chance to transmit the beam without any problem while traveling. Figure 12 shows that the effective beam losses in the Phase-B+ lattice.

The first triplet of HEBT and after bending magnet are the area, which has a lot of particle loss.
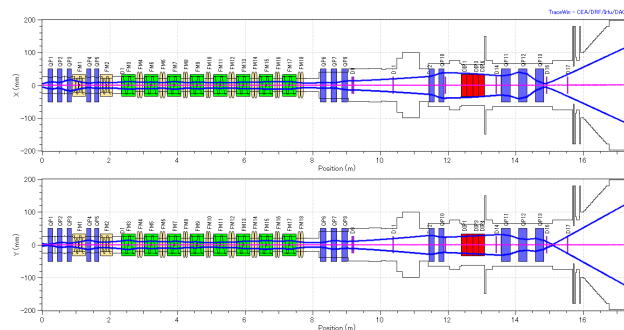
Figure 9: Phase-C lattice transportation of the nominal RFQ extract beam (V=132 kV).
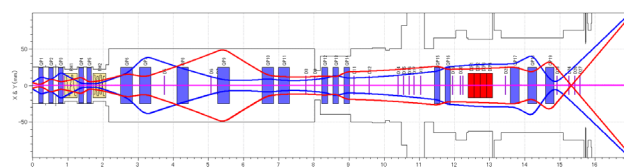
Figure 10: Phase-B+ lattice transportation of the nominal RFQ extract beam (V=132 kV). Blue denotes the horizontal and red denotes the vertical envelopes.
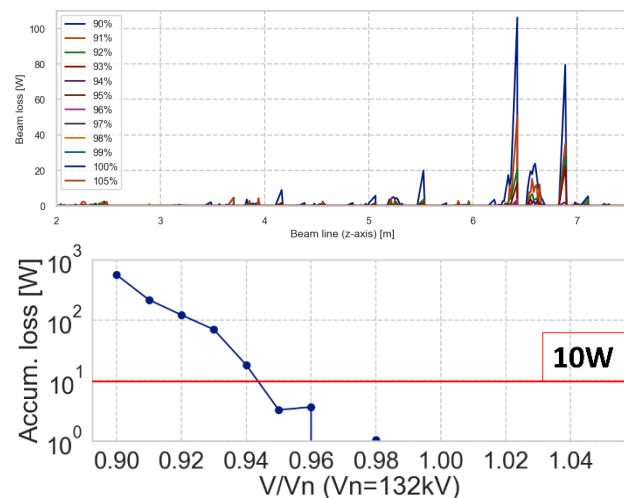
Figure 11: Beam loss pattern in the cryomodule (upper), and RFQ vane voltage vs accumulated beam loss along the cryomodule (lower).
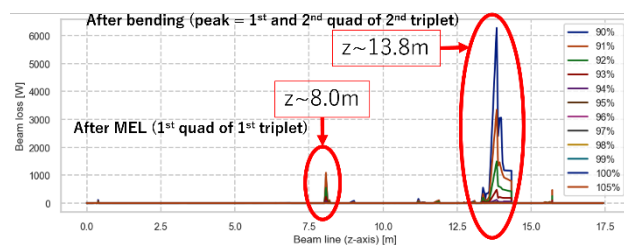
Figure 12: Beam loss pattern in the cryomodule. Upper and lower figure denote the loss of 90–105 percent cases and 96–105 percent cases, respectively.

MEASUREMENT OF MOMENTUM HALO

Time-of-flight Method based on BPM

The Time-of-flight method can estimate the mean energy from measured time duration between two positions of certain bunch. In our BPM based Time-of-flight, time duration can be obtained as the phase difference between two electrodes. Equations (1), (2), and (3) are the relations to derive the mean energy from the relative phase. Here, alignment is assumed to be perfect to the design skeleton, and so errors of the mechanical distance between two electrodes are not considered. An idea, only relative values are used in comparison discussed in later, is also in the background.

$$t_{\text{tof}} = \frac{1}{f_{\text{rf}}} N - \frac{\Delta \varphi}{2\pi} \tag{1}$$

$$\beta = \frac{L}{t_{\text{tof}} \cdot c} \tag{2}$$

$$E_{\text{k}} = m_o c^2 \frac{1}{\sqrt{1 - \beta^2}} - 1 \tag{3}$$

Our BPM digitizer system has very precise synchronization with low-level RF units, which generate accelerating RF signal, via White Rabbit synchronization protocol. As hardware limitation, phases can be provided by 25 MS/s in the highest resolution mode, so we can obtain waveforms of averaged phase over 7 bunches in a pulse. Because signals of 4 BPMs will be sampled by the same clock on the FPGA evaluation board, bunch indexes are the same for series of 4 electrodes. In the measurement, we calculate the relative phase by assuming samples with the same index denote the same batch of bunches.

Calculated energy resolution can be improved less than 0.5 keV with standard errors by taking 50 samples in the second harmonics mode. Because of fluctuation in intra and inter-pulse due to the ECR plasma, chopper, and RFQ voltage transients, averaged values along the flattop part of the beam current are not frozen yet. Here, we are assuming that the effect of transient is partially initialized during rest time of pulsed beam, and so energy derivation based on the Time-of-flight and statistic approaches are applied for each sample index inter-pulses. Figure 13 shows the result of measurement for the last ≈15 µs part of the 60 µs pulse length. The offset including phases and mechanical positions are calibrated at the centre of this short period to make it simulated energy of synchronous particle. So, the measurement is not absolute values here.

All electrodes' combinations show quasi-same values, so we can understand our way could get values with good resolutions and realise to evaluate the intra-pulse fluctuation. This means that, if RFQ entrance condition is fixed, we can consider monitoring the voltage of RFQ to keep acceleration and shaping quality to the downstream linac, by using BPMs.

The measurement will be continued by finding steady region, where phase stability is kept, during the later beam operation.
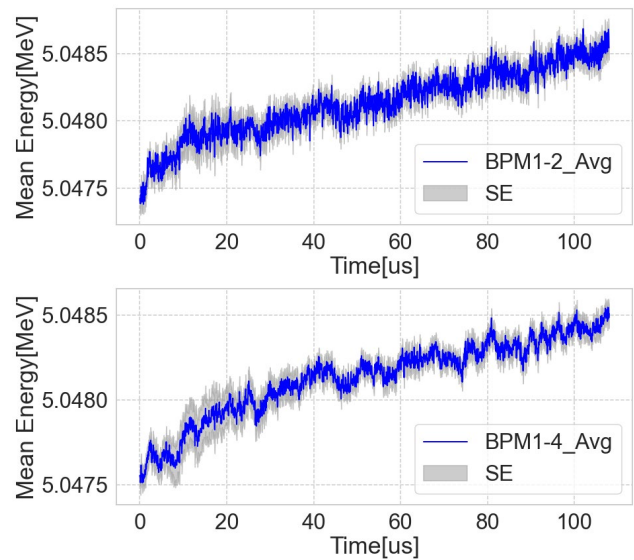
Figure 13: The result of preliminary measurement of mean energy to check the resolution of MEBT BPMs. Gray shadows are areas inside of standard errors for each sample point.

Measurement of Beam Loss near Dipole

Diagnostics system has ionization chamber along the beam line, shown in Fig. 14. And 3H detectors as the neutron counter are prepared along the beam line. According to the tracking simulation, main section of beam losses is spread after bending magnet. In addition to that, the first quadrupole of the first HEBT triplet is also candidate of loss part. Thus, it is good to focus to watch BLoMs No.13, 19, 20, and 21, to compare the loss rate.
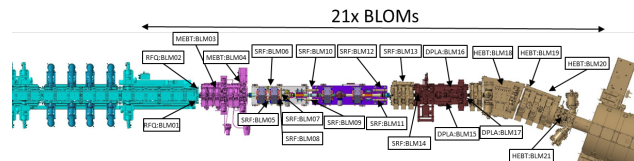
Figure 14: Positions of BLoMs installed along the BT.

SUMMARY

We are discussing to watch the RFQ voltage reduction, by using BPMs and BLoMs, to prepare coming Phase-C commissioning. Simulation studies and trial of the measurement is being conducted and its proceeding is mentioned in this report. According to the simulation, from 94 percent reduced from nominal RFQ voltage, the risk of thermal quench is expected. Mean energy decreasing is started from 94 percent in the RFQ simulation, and beam loss detection can be considered from 95 percent in the TraceWin simulation. This estimation is good threshold to prepare a kind of interlock for the beam extract in the Phase-C and D commissioning. Measurement study is now in progress to know if new operation stopper can be realized on this way.

REFERENCES

[1] J. Knaster *et al.*, "Overview of the IFMIF/EVEDA project", *Nucl. Fusion*, vol. 57, p. 102016, 2017. doi:10.1088/1741-4326/aa6a6a

[2] K. Kondo *et al.*, "Validation of the Linear IFMIF Prototype Accelerator (LIPAc) in Rokkasho", *Fusion Eng. Des.*, vol. 153, p. 111503, 2020. doi:10.1016/j.fusengdes.2020.111503

[3] Y. Shimosaki *et al.*, "Lattice design for 5 MeV – 125 mA CW RFQ operation in LIPAc", in *Proc. IPAC'19*, Melbourne, Australia, May 2019, pp. 977-979. doi:10.18429/JACoW-IPAC2019-MOPTS051

[4] G. Devanz *et al.*, "Manufacturing and validation tests of IFMIF low-beta HWRs", in *Proc. IPAC'17*, Copenhagen, Denmark, May 2017, pp. 942-944. doi:10.18429/JACoW-IPAC2017-MOPVA039

[5] B. Brañas *et al.*, "The LIPAc Beam Dump", *Fusion Eng. Des.*, vol. 127, pp. 127-138, 2018. doi:10.1016/j.fusengdes.2017.12.018

[6] L. Bellan *et al.*, "Acceleration of the high current deuteron beam through the IFMIF-EVEDA beam dynamics performances", in Proc. HB'21, Batavia, IL, USA, Oct. 2021, pp. 197-202. doi:10.18429/JACoW-HB2021-WEDC2

[7] K. Masuda *et al.*, "Commissioning of IFMIF Prototype Accelerator towards CW operation", in *Proc. LINAC'22*, Liverpool, UK, Aug.-Sep. 2022, pp. 319-323. doi:10.18429/JACoW-LINAC2022-TU2AA04

[8] F. Scantamburlo *et al.*, "Linear IFMIF Prototype Accelera-tor (LIPAc) Radio Frequency Quadrupole's (RFQ) RF couplers enhancement towards CW operation at nominal voltage", in *Proc. ISFNT'23*, Sep. 2023, Las Palmas de Gran Canaria, Spain.

[9] A. De Franco *et al.*, "RF conditioning towards continuous wave of the FRQ of the Linear IFMIF Prototype Accelerator", in *Proc. IPAC'23*, Venice, Italy, May 2023, pp. 2345-2348. doi:10.18429/JACoW-IPAC2023-TUPM065

[10] K. Hirosawa *et al.*, "High-Power RF tests of repaired circulator for LIPAc RFQ", in *Proc. PASJ'23*, 2023, Japan.

[11] I. Podadera, J. M. Carmona, A. Ibarra, and J. Molla, "Beam position monitor development for LIPAc", presented at th 8th DITANET Topical Workshop on Beam Position Monitors, CERN, Geneva, Switzreland, Jan. 2012.

[12] I. Podadera *et al.*, "Beam commissioning of beam position and phase monitors for LIPAc", in *Proc. IBIC'19*, Malmö, Sweden, Sep. 2019, pp. 534-538. doi:10.18429/JACoW-IBIC2019-WEPP013

[13] K. Kondo *et al.*, "Neutron production measurement in the 125 mA 5 MeV Deuteron beam commissioning of Linear IFMIF Prototype Accelerator (LIPAc) RFQ", *Nucl. Fusion*, vol. 61, no. 1, p. 116002, 2021. doi:82310.1088/1741-4326/ac233c

[14] S. Kwon *et al.*, "High beam current operation with beam di-agnostics at LIPAc", presented at HB'23, Geneva, Switzerland, Oct. 2023, paper FRC1I2, this conference.

[15] T. Akagi *et al.*, "Achievement of high-current continuous-wave deuteron injector for Linear IFMIF Prototype Accelerator (LIPAc)", to be presented at IAEA FEC'23, London, UK, Oct. 2023. https://www.iaea.org/events/fec2023

[16] "AF4.1.1 SRF Linac Engineering Design Report", Internal note.

[17] L. Bellan *et al.*, "Extraction and low energy beam transport models used for the IFMIF/EVEDA RFQ commissioning", in *Proc. ICIS'21*, TRIUMF, Vancouver, BC, Canada, Sep. 2021. https://indico.cern.ch/event/1027296/